Beam-beam effects investigation and parameters optimization for a circular e^+e^- collider at very high energies

A. Bogomyagkov,* E. Levichev,† and D. Shatilov

Budker Institute of Nuclear Physics SB RAS, Novosibirsk 630090, Russia

(Received 19 December 2013; published 28 April 2014)

Several proposals exist for future circular electron-positron colliders designed for precise measurements of the Higgs boson characteristics and electroweak processes. At very high energies, synchrotron radiation of the particles in a strong electromagnetic field of the oncoming bunch (*beamstrahlung*) becomes extremely important, because of degradation of the beam lifetime and luminosity. We present theoretical calculations of beamstrahlung (including the beam lifetime reduction and the energy spread increase) which are benchmarked against quasi-strong-strong computer simulations. Calculation results are used to optimize TLEP (triple LEP) project (CERN).

DOI: 10.1103/PhysRevSTAB.17.041004 PACS numbers: 29.20.db

I. INTRODUCTION

Design study of high luminosity e^+e^- collider TLEP (triple LEP) for precise measurements of the Higgs boson properties and other experiments at the electroweak scale at CERN has commenced. TLEP will be capable to collide beams in wide center-of-mass energy range from 90 to 350 GeV (with an option up to 500 GeV) with luminosity higher than $5 \times 10^{34}\ \mathrm{cm^{-2}\,s^{-1}}$ [1].

As mentioned in [2], a key issue that limits luminosity and beam lifetime in circular electron-positron colliders with high energy is beamstrahlung, i.e., synchrotron radiation of a lepton deflected by the collective electromagnetic field of the opposite bunch. Because of this radiation, colliding particles of TLEP at high energy could lose so much energy that they are taken out of the momentum acceptance of the accelerator (beam lifetime limitation due to the *single* beamstrahlung). In the beginning of 2013, Telnov estimated lifetime considering single beamstrahlung [3], and set of TLEP parameters using Telnov's formula was given in [4]. For TLEP at low energies, energy loss because of beamstrahlung is not large enough to kick the particles immediately out of the momentum acceptance; however *multiple* beamstrahlung increases beam energy spread and bunch length [5], reducing luminosity owing to the hourglass effect.

We present an analytical approach to calculate the beam lifetime limitation caused by the single beamstrahlung, as well as the energy spread and bunch length increase due to the multiple beamstrahlung. Results of the theoretical predictions are compared with weak-strong beam-beam tracking code LIFETRAC [6], in which the beamstrahlung effect was introduced. A set of new parameters of TLEP with higher luminosity or/and better lifetime is presented for further studies. We considered head-on and crab waist [7] collision schemes.

II. ANALYTICAL CALCULATIONS

A. Beam-beam

The potential of incoming beam is written as [8]

$$U(x,y,s,z) = -\frac{2N_p r_e}{\sqrt{\pi}} \int_0^\infty \frac{\exp\left[-\frac{(x+s2\theta)^2}{2\sigma_x^2+q} - \frac{y^2}{2\sigma_y^2+q} - \frac{\gamma^2(2s-z)^2}{2\gamma^2\sigma_z^2+q}\right]}{\sqrt{(2\sigma_x^2+q)(2\sigma_y^2+q)(2\gamma^2\sigma_z^2+q)}} dq, \quad (1)$$

where r_e is classical electron radius, γ is Lorentz factor, N_p is amount of particles, $\sigma_{x,y,z}$ is horizontal, vertical, and longitudinal beam sizes, 2θ is crossing angle, x, y, s is horizontal, vertical, and longitudinal coordinates, and $z = s - ct$ is the particle's position with respect to the center of the bunch and describes synchrotron oscillations. For simplicity, we will neglect the particle's synchrotron oscillations therefore $z = 0$. Equations of motion are written as

$$y'' = -\frac{\partial U}{\partial y} = -\frac{4N_p r_e}{\sqrt{\pi}} y \int_0^\infty \frac{\exp\left[-\frac{(x+s2\theta)^2}{2\sigma_x^2+q} - \frac{y^2}{2\sigma_y^2+q} - \frac{\gamma^2(2s)^2}{2\gamma^2\sigma_z^2+q}\right]}{\sqrt{(2\sigma_x^2+q)(2\sigma_y^2+q)^3(2\gamma^2\sigma_z^2+q)}} dq, \quad (2)$$

*Also at Novosibirsk State University, Novosibirsk 630090, Russia.
A.V. Bogomyagkov@inp.nsk.su
†Also at Novosibirsk State Technical University, Novosibirsk 630073, Russia.

$$x'' = -\frac{\partial U}{\partial x} = -\frac{4N_p r_e}{\sqrt{\pi}} x \int_0^\infty \frac{\exp\left[-\frac{(x+s2\theta)^2}{2\sigma_x^2+q} - \frac{y^2}{2\sigma_y^2+q} - \frac{\gamma^2(2s)^2}{2\gamma^2\sigma_z^2+q}\right]}{\sqrt{(2\sigma_x^2+q)^3(2\sigma_y^2+q)(2\gamma^2\sigma_z^2+q)}} dq. \tag{3}$$

In order to calculate effective interaction length L and mean bending radius $\rho_{x,y}$ in hard edge approximation we will neglect $\sigma_{x,y}$ dependence on s and find expected values of vertical $\Delta y'$ and horizontal $\Delta x'$ kicks. We also assume that $\sigma_x \gg \sigma_y$. After calculations we obtained

$$\langle|\Delta y'|\rangle_{y,x+s2\theta=0} \approx \sqrt{\frac{\pi}{2}} \frac{N_p r_e}{\gamma\sigma_x\sqrt{1+\phi^2}}, \tag{4}$$

$$\langle|\Delta x'|\rangle_{x,y=0} \approx \frac{\log\left(\frac{\sqrt{2}+1}{\sqrt{2}-1}\right)}{\sqrt{\pi}} \frac{N_p r_e}{\gamma\sigma_x\sqrt{1+\phi^2}}, \tag{5}$$

where $\phi = \sigma_z \tan(\theta)/\sigma_x$ is Piwinski parameter, $\langle\rangle$ means expected value with respect to the first subindex while the other one satisfies the condition in the second. The inverse bending radius in the corresponding plane is calculated as

$$\frac{1}{\rho_y} = \langle|y''|\rangle_{y,x+s2\theta=0} \approx \frac{N_p r_e}{\gamma\sigma_z\sigma_x}, \tag{6}$$

$$\frac{1}{\rho_x} = \langle|x''|\rangle_{x,y=0} \approx \frac{\sqrt{2}}{\pi} \log\left(\frac{\sqrt{2}+1}{\sqrt{2}-1}\right) \frac{N_p r_e}{\gamma\sigma_z\sigma_x}. \tag{7}$$

Finally effective interaction length in each plane is

$$L = L_x = L_y = \frac{\langle|\Delta y'|\rangle_{y,x+s2\theta=0}}{\langle|y''|\rangle_{y,x+s2\theta=0}} = \frac{\langle|\Delta x'|\rangle_{x,y=0}}{\langle|x''|\rangle_{x,y=0}} = \sqrt{\frac{\pi}{2}} \frac{\sigma_z}{\sqrt{1+\phi^2}}. \tag{8}$$

Since $\log(\frac{\sqrt{2}+1}{\sqrt{2}-1})\sqrt{2}/\pi \approx 0.8$ for our estimation we will count horizontal and vertical bending radii as equal:

$$\frac{1}{\rho_x} \approx \frac{1}{\rho_y} \approx \frac{N_p r_e}{\gamma\sigma_z\sigma_x}. \tag{9}$$

B. Beamstrahlung

Following the approach given in [3] we calculated the amount of emitted photons (10) and beam lifetime (11). The only difference is that we do not make an assumption of 10% of the particles experiencing the maximum field, but use average values calculated in the previous paragraph:

$$N(u > \eta E_0) = \frac{3}{4\sqrt{\pi}} \sqrt{\frac{\alpha r_e}{\eta}} \exp\left(-\frac{2}{3}\frac{\eta\alpha\rho}{r_e\gamma^2}\right) \frac{L\gamma^2}{\rho^{3/2}}, \tag{10}$$

$$\tau_{bs} = \frac{1}{f_0 N N_{ip}} = \frac{1}{f_0 N_{ip}} \frac{4\sqrt{\pi}}{3} \sqrt{\frac{\eta}{\alpha r_e}} \exp\left(\frac{2}{3}\frac{\eta\alpha\rho}{r_e\gamma^2}\right) \frac{\rho^{3/2}}{L\gamma^2}, \tag{11}$$

where α is fine-structure constant and N_{ip} is number of interaction points (IPs).

The difference from Telnov's calculations is in estimation of interaction length L (8),

$$L_{\text{Telnov}} = \frac{\sigma_z}{2}, \tag{12}$$

and in expression for the total bending radius ρ [ρ_x and ρ_y from (9)],

$$\frac{1}{\rho} = \sqrt{\frac{1}{\rho_x^2} + \frac{1}{\rho_y^2}} \approx \frac{N_p r_e}{\gamma\sigma_x\sigma_z}\sqrt{2}, \tag{13}$$

$$\frac{1}{\rho_{\text{Telnov}}} \approx \frac{N_p r_e}{\gamma\sigma_x\sigma_z} 2. \tag{14}$$

The radiation integrals which define energy spread and bunch length [9] are modified according to

$$\Delta I_2 = \left(\frac{L}{\rho_x^2} + \frac{L}{\rho_y^2}\right) N_{ip}, \tag{15}$$

$$\Delta I_3 = \frac{L}{\rho^3} N_{ip}, \tag{16}$$

where N_{ip} is a number of interaction points.

It is convenient to rewrite the expression for bending radius using beam-beam tune shift ξ_y (taken from [10]) and interaction length L,

$$\xi_y = \frac{N_p r_e}{2\pi\gamma\epsilon_y} \frac{\sigma_y}{\sigma_x} \frac{1}{\sqrt{1+\phi^2}}, \tag{17}$$

$$\frac{1}{\rho} = \xi_y \sqrt{\frac{\epsilon_y}{\beta_y}} \frac{2\pi^{3/2}}{L}, \tag{18}$$

where ϵ_y and β_y are vertical emittance and beta function at IP respectively.

At last, we obtain the expression for the beam lifetime:

$$\tau_{bs} = \frac{1}{f_0}\frac{4\sqrt{\pi}}{3}\sqrt{\frac{\eta}{\alpha r_e}}\exp\left(\frac{2}{3}\frac{\eta\alpha}{r_e\gamma^2}\times\frac{\gamma\sigma_x\sigma_z}{\boldsymbol{\sqrt{2}}r_eN_p}\right) \times\frac{\boldsymbol{\sqrt{2}}}{\sqrt{\pi}\sigma_z\gamma^2}\left(\frac{\gamma\sigma_x\sigma_z}{\boldsymbol{\sqrt{2}}r_eN_p}\right)^{3/2}, \quad (19)$$

where $N_{ip} = 1$ and bold symbols are showing the difference from the expression given in [3],

$$\tau_{\mathrm{bs,Telnov}} = \frac{\mathbf{10}}{f_0}\frac{4\sqrt{\pi}}{3}\sqrt{\frac{\eta}{\alpha r_e}} \times\exp\left(\frac{2}{3}\frac{\eta\alpha}{r_e\gamma^2}\times\frac{\gamma\sigma_x\sigma_z}{\mathbf{2}r_eN_p}\right)\frac{\mathbf{2}}{\sigma_z\gamma^2}\left(\frac{\gamma\sigma_x\sigma_z}{\mathbf{2}r_eN_p}\right)^{3/2}. \quad (20)$$

Beamstrahlung influence makes the bunch longer, and also depends on the bunch length. In order to take into account this effect, we calculated synchrotron radiation integrals [(15) and (16)] and bending radius (13) in several (about 50) repeated iterations, where the bunch length was assigned a geometric mean of its values on the previous two steps; thus the equilibrium was found. Using new values for bunch length, radius and interaction length we calculated beam lifetime from expression (11).

III. THE MODEL USED IN BEAM-BEAM SIMULATIONS

To track a test particle through IP, the opposite (strong) bunch is represented by a number of thin slices. The trajectory's bending radius for each slice can be estimated as

$$\rho \approx \frac{\Delta s}{\Delta p/p}, \quad (21)$$

where Δs is effective slice width and Δp is the transverse component of beam-beam kick. The radiation spectrum corresponds to normal synchrotron radiation from a bending magnet if the following condition is satisfied:

$$\left(\frac{\Delta p}{p}\right)_{\mathrm{total}} \gg \frac{1}{\gamma}. \quad (22)$$

Here $(\Delta p/p)_{\mathrm{total}}$ stays for the entire bunch (not a slice) and can be estimated as $4\pi\xi\sigma' \geq 10^{-4}$. The given condition is always satisfied at the large energies (e.g., TLEP, $\gamma \geq 10^5$). The critical energy of radiation u_c (in units of mean beam energy $E_0 = \gamma_0 mc^2$) is

$$\frac{u_c}{E_0} = \frac{3}{2}\gamma_0^2\left(1+\frac{\delta_E}{E_0}\right)^3\frac{r_e}{\alpha\rho}, \quad (23)$$

where δ_E is the particle's energy deviation. Hereafter, the energy of emitted photons is always normalized with respect to critical energy u_c. The spectrum density of radiation is

$$\frac{d}{dt}n(u/u_c) = \frac{\sqrt{3}}{2\pi}\alpha\gamma\frac{c}{\rho}\int_{u/u_c}^{\infty}K_{5/3}(x)dx\,d\left(\frac{u}{u_c}\right). \quad (24)$$

Note that at relatively small energies, where (22) becomes invalid, u_c drops significantly and we can neglect the whole effect of beamstrahlung, therefore there is no need to be concerned about the spectrum. Taking into account the time of interaction, $\Delta t = \Delta s/c$, we obtain the (average) number of emitted photons in a small interval of spectrum:

$$\Delta n(u/u_c) = \frac{\sqrt{3}}{2\pi}\alpha\gamma\frac{\Delta p}{p}\int_{u/u_c}^{\infty}K_{5/3}(x)dx\,\Delta\left(\frac{u}{u_c}\right). \quad (25)$$

The actual number of emitted photons is given by Poisson distribution. For tracking purposes we replace the continuous spectrum by a sequence of discrete lines, from 0.01 to 20 with a step of 0.01 (all in units of u_c)—2000 in total. The limits were chosen from the conditions that the radiation power below the lower and probability of photon emission above the upper are negligible. The step between the lines is small enough to adequately represent the spectrum. Since the critical energy u_c also depends on the actual particle's trajectory, the overall spectrum of emitted photons in simulations will be continuous regardless of being discrete in units of u_c. Considering randomness (and rather low probability) of photon emission in any given interval of $\Delta(u/u_c)$, we conclude that our spectrum simplifications will not affect the final results.

Hence, we have $\Delta(u/u_c) = 0.01$ in (25) and our lines correspond to spectrum intervals of $0.005 \div 0.015$ (1st), $0.015 \div 0.025$ (2nd), etc. The integrals of $K_{5/3}(x)$ were calculated once and written in a static table for all 2000 points. The sum of all these values is responsible for the total (average) number of emitted photons,

$$\bar{n} = \frac{\sqrt{3}}{200\pi}\alpha\gamma\frac{\Delta p}{p}\sum_{m=1}^{2000}\int_{m/100}^{\infty}K_{5/3}(x)dx. \quad (26)$$

The overall simulation algorithm is as follows. First, $\Delta p/p$ is calculated for each particle after passing a single slice of the opposite bunch. Second, the u_c is calculated from (21) and (23), and $\bar{n}$—from (26). Then, the actual number of emitted photons N_{ph} (which can be zero) is obtained from the Poisson distribution with parameter $\bar{n}$, using random number uniformly distributed in the interval of $[0, 1]$. The energy of each particular photon is defined according to the relative probabilities [which are proportional to integrals of $K_{5/3}(x)$] for different spectrum lines, using another random number. In total, the random number

TABLE I. Main parameters from the 2013 workshop at CERN [4].

	Z	W	H	t		ttH, ZHH
E_{beam}, GeV	45	80	120	175		250
Current [mA]	1440	154	29.8	6.7		1.6
N_{bunches}	7500	3200	167	160	20	10
$N_{\mathrm{particles}}[10^{11}]$	4.0	1.0	3.7	0.88	7.0	3.3
$\epsilon_x[\mathrm{nm}]/\epsilon_y[\mathrm{pm}]$	29.2/60	3.3/17	7.5/15	2/2	16/16	4/4
$\beta_x^*[\mathrm{m}]/\beta_y^*[\mathrm{mm}]$	0.5/1	0.2/1	0.5/1	1/1		1/1
$\sigma_z[\mathrm{mm}]$	2.93	1.98	2.11	0.77	1.95	1.81
N_{ip}	4					
F_{hg} hourglass	0.61	0.71	0.69	0.90	0.71	0.73
$L/\mathrm{IP}[10^{32}\mathrm{cm}^{-2}\mathrm{s}^{-1}]$	5860	1640	508	132	104	48
ξ_x/IP	0.068	0.086	0.094	0.057		0.075
ξ_y/IP	0.068	0.086	0.094	0.057		0.075
$\tau_L[\mathrm{s}]$	5940	2280	1440	1260	1560	780
$\tau_{\mathrm{bs}}(\eta=2\%)[\mathrm{s}]$	$>10^{25}$	$>10^{6}$	2280	840	126	18
$\tau_{\vert\vert}$	1319	242	72	23		8
$f_s[\mathrm{kHz}]$	0.77	0.19	0.27	0.14	0.29	0.266
$P_{\mathrm{SR}}[\mathrm{MW}]$	50	50	50	50	50	50

generator is called $N_{\mathrm{ph}}+1$ times for each particle-slice interaction.

It is noteworthy, beamstrahlung simulations are not affected by the number of slices N_{sl}—if it is large enough to correctly represent the opposite bunch. For example, further increase of N_{sl} leads to proportional decrease of both Δs and $\Delta p/p$, while ρ and u_c remain unchanged. The total number of emitted photons also does not change: $\bar{n}$ for each slice decreases with $\Delta p/p$, but it is compensated by N_{sl} increase.

TLEP has four interaction points (Table I), therefore lattice is assumed to possess fourfold symmetry and we chose fractional betatron phase advances between IPs (0.53, 0.57).

Simulations were performed by weak-strong beam-beam tracking code LIFETRAC [6]. Beamstrahlung influence makes the bunch longer, and also depends on the bunch length. Therefore we used the quasi-strong-strong method, where in the several repeated iterations the weak and strong bunches exchanged their roles and the length of the strong bunch was assigned geometric mean of strong and weak bunches; thus the equilibrium of the bunch length was found.

IV. COMPARISON OF OUR RESULTS WITH PREVIOUS

Initially, we compared our simulation and analytical formula (19) with the calculations made in CERN. We used a table of parameters for TLEP given at the 2013 workshop [4], which are summarized in Table I. Analytical calculations, simulations by LIFETRAC and given parameters from Table I of luminosity, beam lifetime, bunch length, energy spread are plotted in Figs. 1, 2, 4, and 5 respectively. In all figures CERN stands for CERN calculations from the base table (Table I), LIFETRAC full stands for quasi-strong-strong simulations by LIFETRAC with full spectrum of beamstrahlung, LIFETRAC threshold stands for weak-strong simulations by LIFETRAC where only photons with energy higher than energy acceptance are taken into account, meaning that bunch length does not increase (similar to Telnov's approach), and analytical is calculations by (19) including bunch lengthening [(15) and (16)]. We understand that the model used in simulations does not implement all the effects, but in the present paper we consider simulations as the most accurate calculations and compare everything against them. Luminosity calculations by different approaches are consistent except the TLEPZ scenario; the difference for the latter is because analytical and probably CERN calculations did not consider beam-beam effects but beamstrahlung. As it will be shown later, bunch lengthening

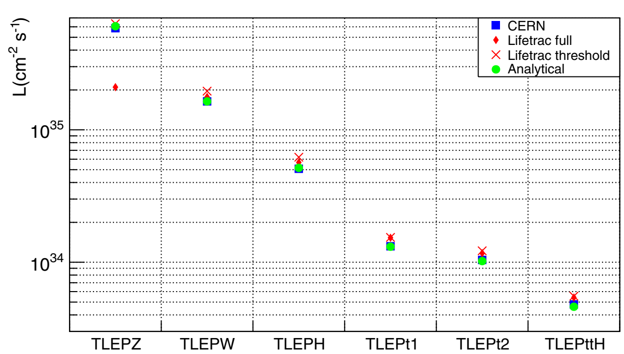

FIG. 1. Luminosity for different scenarios of TLEP operation. Blue squares are taken from Table I, red diamonds are LIFETRAC results with full spectrum of beamstrahlung, red crosses are LIFETRAC results if beamstrahlung is considered for emission of photons with energy higher than acceptance, green dots are our analytical calculations.

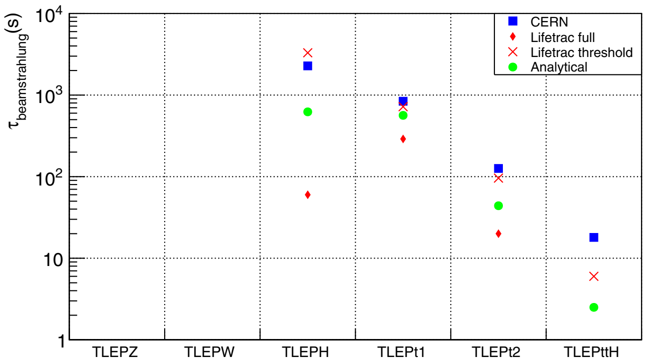

FIG. 2. Beam lifetime for different scenarios of TLEP operation. Blue squares are taken from Table I, red diamonds are LIFETRAC results with full spectrum of beamstrahlung, red crosses are LIFETRAC results if beamstrahlung is considered for emission of photons with energy higher than acceptance, and green dots are our analytical calculations. Lifetimes for TLEPZ and TLEPW are so large, therefore not plotted.

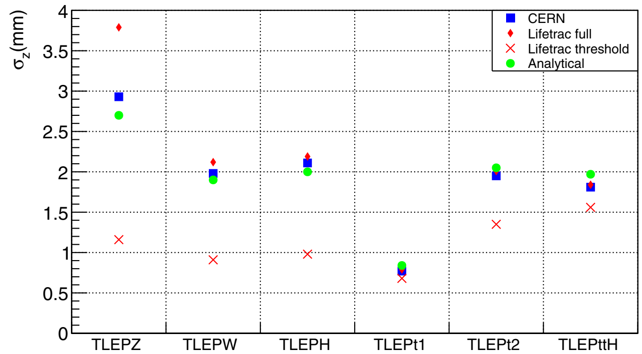

FIG. 4. Bunch length for different scenarios of TLEP operation. Blue squares are taken from Table I, red diamonds are LIFETRAC results with full spectrum of beamstrahlung, red crosses are LIFETRAC results if beamstrahlung is considered for emission of photons with energy higher than acceptance, and green dots are our analytical calculations.

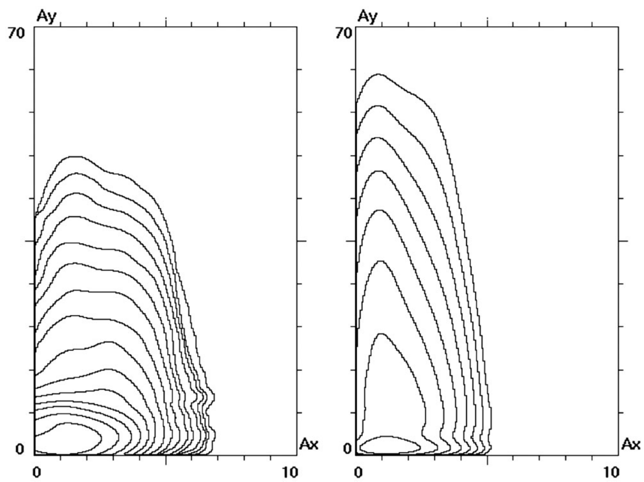

FIG. 3. Equilibrium beam distribution in the plane of normalized betatron amplitudes for TLEPZ. Left is without beamstrahlung, right is with beamstrahlung. The density between successive contour lines drops by a factor of e.

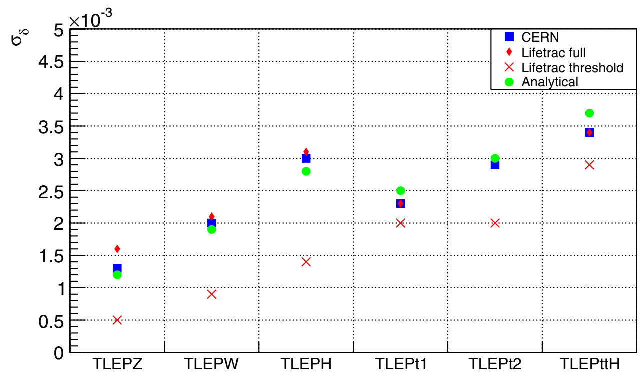

FIG. 5. Energy spread for different scenarios of TLEP operation. Blue squares are taken from Table I, red diamonds are LIFETRAC results with full spectrum of beamstrahlung, red crosses are LIFETRAC results if beamstrahlung is considered for emission of photons with energy higher than acceptance, and green dots are our analytical calculations.

due to beamstrahlung is significant in the TLEPZ scenario, because it leads to a huge hourglass with a result of a blown-up beam in the vertical plane. To illustrate this, we compared transverse beam distributions calculated by LIFETRAC without beamstrahlung (left) and with beamstrahlung (right) in Fig. 3.

On the contrary to the luminosity calculations agreement, the beam lifetime (Fig. 2) given by LIFETRAC full is consistently smaller than analytical calculations because in the latter case particles energy distribution was neglected. However, particle with energy deviation may lose a lesser amount of energy in order to be lost. Additionally, beam energy spread (Fig. 5) becomes larger and energy acceptance of the accelerator shrinks to only 7–10 rms of energy distribution. Also, analytical calculations do not include beam size dependence on longitudinal position (hourglass). The LIFETRAC threshold simulations of beam lifetime (red crosses in Fig. 2) correspond well to initial CERN results (blue squares), since they conform to the assumption made by Telnov. Our analytical calculations (green dots in Fig. 2) are closer to LIFETRAC full, especially at TLEPttH.

Bunch length (Fig. 4) and energy spread (Fig. 5) for LIFETRAC threshold (red crosses) do not change in calculations because of made assumptions. The discrepancy of bunch length and energy spread between scenarios (red crosses) corresponds to different optics.

The performed comparison shows that accurate simulation gives smaller luminosity at TLEPZ, smaller beam lifetime in all scenarios. At TLEPttH the beam lifetime is so small (2 sec by LIFETRAC full and by our analytics) that the given scenario is not feasible.

V. NEW SET OF PARAMETERS

Luminosity for flat beams is given (without hourglass and dynamical beta) by the well-known expression

$$\mathcal{L} = \frac{\gamma}{2er_e} I \frac{\xi_y}{\beta_y}, \tag{27}$$

where I is a full beam current (limited by synchrotron energy loss), e is electron charge, ξ_y is vertical beam-beam tune shift, and β_y is beta function at IP. The given value of $\beta_y = 1$ mm is already small, further decrease is not reasonable. Hence, luminosity increase is only possible by making ξ_y larger.

Analytical calculations and simulation show that beam-beam effects for TLEP are determined by several factors, quantitative relations between which greatly depend on energy. At high energies (TLEPH and higher) beamstrahlung becomes a main factor which determines beam lifetime. The only way to decrease beamstrahlung influence (11) is to increase ρ (18). Vertical emittance ϵ_y is chosen at the minimum value defined by coupling; increase of β_y and decrease of ξ_y are not desirable because of luminosity degradation (27). Therefore, we need to increase interaction length L (8) (in head-on collision—by increasing the bunch length). We will assume that the bending radius of beamstrahlung should rise proportionally to energy (or even faster) in order to keep an acceptable lifetime at high energies.

Another influence of beamstrahlung is increase of the beam energy spread and of the bunch length. Oddly enough, this effect is important at low energies (TLEPZ and TLEPW) but not at high energies. This happens because relative critical energy u_c/E_0 of synchrotron radiation in dipoles rises as γ^2 (23), since bending radius in dipoles does not change, but of beamstrahlung as γ. The number of photons in both cases is proportional to energy. This is valid for beamstrahlung because interaction length changes with energy in the same manner as bending radius. Thus, the relative input of beamstrahlung in energy spread falls with energy increase.

An apparent paradox of why then at high energies beam lifetime is limited by beamstrahlung is solved by noticing that in spite of faster rise of u_c with energy for conventional synchrotron radiation, beamstrahlung u_c is still significantly higher at all energies, because bending radius in beamstrahlung is at least 2 orders of magnitude smaller than one of dipoles. Hence, energy of the photons emitted in IP is by 2 orders of magnitude higher (but amount of them is smaller). Though, beam lifetime is determined by probability to radiate single photon with high energy, which comes from beamstrahlung.

Increasing the bunch length could have a negative effect. When $\beta_y \ll \sigma_z$ (head-on collisions) hourglass increases the actual beam-beam tune shift and makes synchrobetatron resonances stronger; both effects lead to beam blowup. On the other hand, strong damping at high energies (TLEPH and higher) counteracts the negative influence of synchrobetatron resonances. Also, the utmost value of beam-beam tune shift at high energies is relatively small because it is determined by beamstrahlung rather than conventional beam-beam effects.

At low energies, where damping is weaker and bunch lengthening is stronger, hourglass leads to serious consequences for equilibrium beam distribution in the vertical plane (Fig. 3). The crab waist collision scheme [7] allows one to solve this problem. Interaction with a large Piwinski parameter permits to make $\beta_y \ll \sigma_z$ without negative influence of hourglass; then crab sextupoles allow to obtain record high beam-beam tune shift ξ_y. Yet, at high energies crab waist is almost useless because ξ_y is already limited by beamstrahlung.

Considering our speculations, we propose the following approach to decide on TLEP parameters at different energies. At the foundation of the approach is a desire to have the same lattice at all energies and to obtain maximum luminosity with satisfying beam lifetime. A set of parameters for TLEPH from Table I is used as a base. However, we increased synchrotron bunch length to 4.9 mm from the original 0.98 mm (mainly by lowering rf frequency), kept energy spread the same of 1.4×10^{-3}. The other scenarios are scaled with respect to energy in emittance, energy spread and energy loss. Bunch length is scaled with energy and adjusted by varying rf amplitude, paying due attention to the size of the rf bucket ($\delta_{\mathrm{rf,bucket}}$).

At low energies, in order to implement the crab waist collision scheme, we introduced a relatively moderate crossing angle of $2\theta = 30$ mrad. The chosen value provides interaction length L approximately equal to vertical beta function ($\beta_y = 1$ mm) at TLEPZ and TLEPW. We kept the same crossing angle for other scenarios in order to preserve geometry of the interaction region. The bunch length was chosen from the following considerations. The ratio between vertical and horizontal tune shifts is given by the formula [10]

$$\frac{\xi_y}{\xi_x} = \sqrt{\frac{\epsilon_x \beta_y}{\epsilon_y \beta_x}(1 + \phi^2)}. \tag{28}$$

In order to achieve large $\xi_y \sim 0.18$ in the crab waist scheme, we need to ensure that the beam-beam footprint does not cross strong betatron and synchrobetatron resonances of low orders. It follows that ξ_x should be small, for example $\xi_x \lesssim 0.03$. On the other hand, it would be difficult to obtain $\epsilon_y \lesssim 1$ pm. Therefore the Piwinski parameter (taking into account bunch lengthening due to beamstrahlung) must be rather large: $\phi > 10$, which gives requirement on the equilibrium bunch length: $\sigma_z \sim \phi \sigma_x/\theta$. This is the reason why we decided to increase σ_z in the base scenario TLEPH. Besides, at low energies additional bunch lengthening is achieved by lowering rf amplitude, which is also advantageous because of synchrotron tune decrease. In this way we

TABLE II. A new set of parameters with crossing angle and crab waist.

	Z	W	H	t	ttH, ZHH
Π[km]			100		
2θ[mrad]			30		
Current [mA]	1431	142	29	6.3	1.4
N_{bunches}	29791	739	127	33	6
$N_{\mathrm{particles}}[10^{11}]$	1	4	4.7	4	5
$\epsilon_x[\mathrm{nm}]/\epsilon_y[\mathrm{pm}]$	0.14/1	0.44/2	1/2	2.1/4.25	4.34/8.68
$\beta_x^*[\mathrm{m}]/\beta_y^*[\mathrm{m}]$			0.5/0.001		
F_{rf}[MHz]			300		
V_{rf}[GV]	0.54	1.35	3.6	11.4	34.2
ν_{syn}	0.062	0.072	0.092	0.124	0.124
$\delta_{\mathrm{rf,bucket}}$	5.9	5.9	6	6.1	2.6
Momentum compaction α			2×10^{-5}		
$\sigma_{s,\mathrm{syn}}$[mm]	2.7	4.1	4.9	5.3	7.5
$\sigma_{\delta,\mathrm{syn}}[10^{-3}]$	0.5	0.9	1.4	2	2.9
σ_z[mm]	5.9	9.1	8.2	6.6	8
$\sigma_\delta[10^{-3}]$	1.2	2.1	2.4	2.6	3.1
ϕ	10.6	9.1	5.5	3	2.6
L[mm]	0.7	1.2	1.8	2.6	3.6
F_{hg} hourglass	0.94	0.86	0.78	0.7	0.61
$L/\mathrm{IP}[10^{32}\ \mathrm{cm^{-2}\ s^{-1}}]$	21200	3640	924	134	18
ξ_x/IP	0.032	0.031	0.029	0.024	0.014
ξ_y/IP	0.175	0.187	0.16	0.077	0.038
τ_L[s]	2300	1300	1100	1800	2900
$\tau_{\mathrm{bs}}(\eta=2\%)$[s]	$>10^{19}$	$>10^{6}$	40000	5500	2700
$\tau_{\|\|}$	1338	238	70	22	7
$U_{\mathrm{loss,SR}}$[GeV/turn]	0.03	0.3	1.7	7.7	32
P_{SR}[MW]	50	50	50	49.1	46.3

obtain the desired ξ_y/ξ_x ratio. Then, bunch population N_p is set to provide the required values for tune shifts.

At high energies, where lifetime is restricted by beamstrahlung, we should increase ρ in order to reduce u_c. Since we have to keep ξ_y as large as possible for higher luminosity, the only way is increasing the interaction length L (18). In our scheme L goes up linearly with energy as it is proportional to σ_x. On the other hand, the negative influence of huge hourglass ($L/\beta_y > 3$ for TLEPttH) is restricted owing to very strong damping. It is worth mentioning that, for flat bunches, beamstrahlung dependence on vertical beam size is rather weak. Therefore bunch population N_p is defined from the requirement on acceptable beamstrahlung lifetime. Then, in order to obtain maximum ξ_y (and luminosity), ϵ_y should be minimized. However, we believe that it would be hard to obtain the coupling parameter $\epsilon_y/\epsilon_x < 0.002$, and this relation defines the achievable ξ_y. Since the Piwinski parameter at these scenarios is not small ($\phi > 2.5$), crab sextupoles still remain helpful and decrease vertical beam blowup because of beam-beam effects.

For all scenarios, the number of bunches was calculated so that the total power loss does not exceed 50 MW. Crossing angle in all cases helps to facilitate separation of the bunches and accommodation of the final focus elements.

The new set of parameters is given in Table II. Our proposal compared against LIFETRAC full for original CERN set of parameters (Figs. 6 and 7) gives 10 times higher luminosity at TLEPZ, 2 times higher luminosity at TLEPW and 1.6 times higher at TLEPH. For TLEPt and TLEPttH the luminosity is lower, but we got acceptable beamstrahlung lifetime. On the figures LIFETRAC full stands for simulation of the original table of parameters

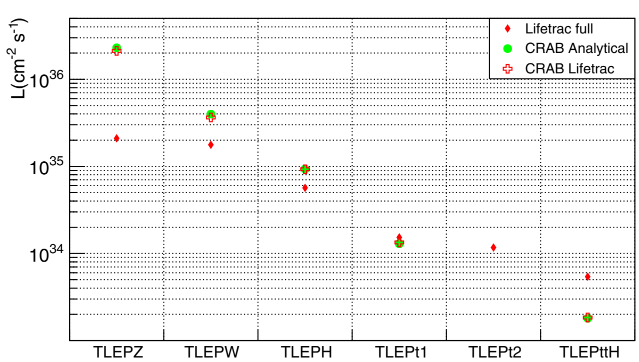

FIG. 6. Luminosity for different scenarios of TLEP operation. Red diamonds and red empty crosses are LIFETRAC simulations with full spectrum of beamstrahlung for Tables I and II, correspondingly; green dots are analytical calculations for the latter case.

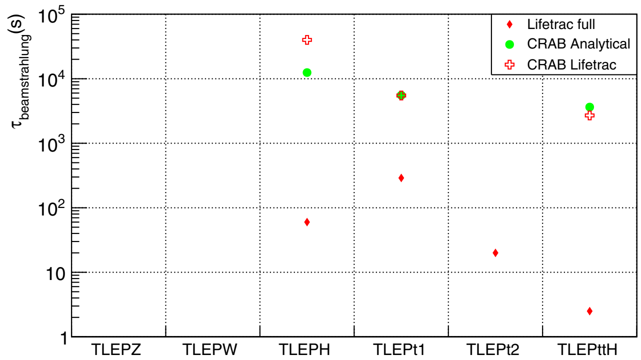

FIG. 7. Beam lifetime for different scenarios of TLEP operation. Red diamonds and red empty crosses are LIFETRAC simulations with full spectrum of beamstrahlung for Tables I and II, correspondingly; green dots are analytical calculations for the latter case.

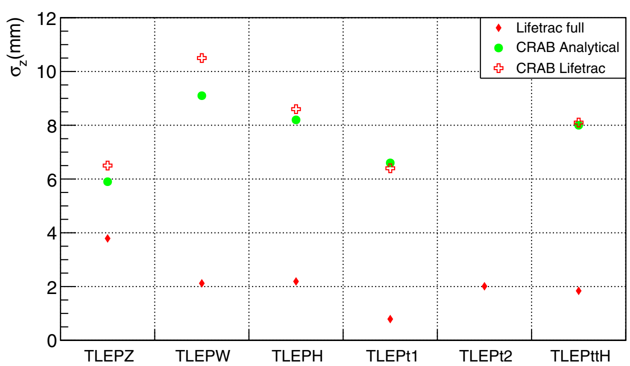

FIG. 8. Bunch length for different scenarios of TLEP operation. Red diamonds and red empty crosses are LIFETRAC simulations with full spectrum of beamstrahlung for Tables I and II, correspondingly; green dots are analytical calculations for the latter case.

(Table I, red diamonds), crab analytical and crab LIFETRAC full are calculations (green dots) and simulations (red empty crosses) respectively, for the new set (Table II).

The bunch length and energy spread are shown in Figs. 8 and 9. Analytical calculations correspond well with LIFETRAC simulations at TLEPH, TLEPt and TLEPttH. Discrepancy at TLEPZ and TLEPW happens because analytical calculations do not consider horizontal and vertical emittance increase owing to beam-beam effects.

VI. CONCLUSION

We have considered different aspects of the beamstrahlung influence on the parameters of the high-energy high-luminosity e^+e^- storage ring collider TLEP operating in the energy range from Z-pole up to the $t\bar{t}$ threshold.

Accurate consideration of beamstrahlung influence requires quasi-strong-strong or strong-strong simulation

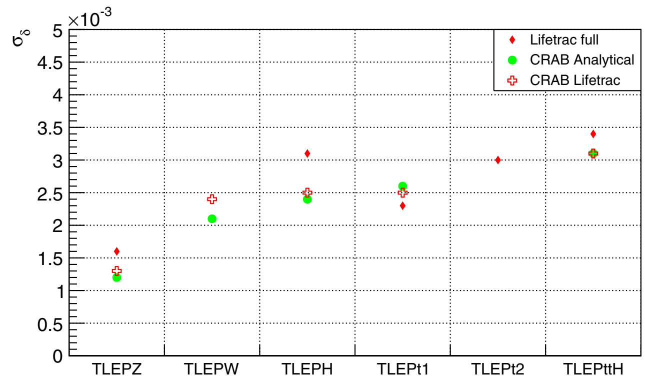

FIG. 9. Energy spread for different scenarios of TLEP operation. Red diamonds and red empty crosses are LIFETRAC simulations with full spectrum of beamstrahlung for Tables I and II, correspondingly; green dots are analytical calculations for the latter case.

with damping and noise excitation. An analytical approach does not consider all the effects, however gives sufficient estimation.

We propose a novel approach to define TLEP parameters and a new set of parameters considering all the effects mentioned above. Our scheme has the same lattice for all scenarios, with large Piwinski parameter and crab waist, which allowed us to increase luminosity several times for low energies and increase beam lifetime to acceptable values at high energies.

ACKNOWLEDGMENTS

We would like to thank V. Telnov, M. Koratzinos, and F. Zimmermann for fruitful discussions. The work is supported by Russian Ministry of Education and Science.

[1] A. Blondel and F. Zimmermann, arXiv:1112.2518v2.
[2] J. Augustin, N. Dikansky, Y. Derbenev, J. Rees, B. Richter *et al.*, eConf **C781015**, 009 (1978).
[3] V. I. Telnov, Phys. Rev. Lett. **110**, 114801 (2013).
[4] F. Zimmermann, http://indico.cern.ch/conferenceDisplay.py?confId=272526.
[5] K. Ohmi, at the 5th TLEP Workshop (TLEP13) (2013).
[6] D. Shatilov, Part. Accel. **52**, 65 (1996).
[7] P. Raimondi, at the 2nd Workshop on Super B factory, LNF-INFN, Frascati, 2006.
[8] A. Zholents, Lect. Notes Phys. **400**, 321 (1992).
[9] R. H. Helm, M. J. Lee, P. Morton, and M. Sands, IEEE Trans. Nucl. Sci. **20**, 900 (1973).
[10] D. Shatilov and M. Zobov, ICFA Beam Dyn. Newsletter **37**, 99 (2005).